Current Topics

Assembly of Nitrogenase MoFe Protein[†]

Yilin Hu,* Aaron W. Fay, Chi Chung Lee, Janice Yoshizawa, and Markus W. Ribbe*

Department of Molecular Biology and Biochemistry, University of California, Irvine, California 92697-3900

Received December 20, 2007; Revised Manuscript Received January 18, 2008

ABSTRACT: Assembly of nitrogenase MoFe protein is arguably one of the most complex processes in the field of bioinorganic chemistry, requiring, at least, the participation of *nifS*, *nifU*, *nifB*, *nifE*, *nifN*, *nifV*, *nifQ*, *nifZ*, *nifH*, *nifD*, and *nifK* gene products. Previous genetic studies have identified factors involved in MoFe protein assembly; however, the exact functions of these factors and the precise sequence of events during the process have remained unclear until the recent characterization of a number of assembly-related intermediates that provided significant insights into this biosynthetic "black box". This review summarizes the recent advances in elucidation of the mechanism of FeMoco biosynthesis in four aspects: (1) the *ex situ* assembly of FeMoco on NifEN, (2) the incorporation of FeMoco into MoFe protein, (3) the *in situ* assembly of P-cluster on MoFe protein, and (4) the stepwise assembly of MoFe protein.

Nitrogenase is a complex metalloenzyme that catalyzes one of the most remarkable chemical transformations in biological systems: the ATP-dependent reduction of atmospheric dinitrogen to bioavailable ammonia (for recent reviews, see refs *1–6*). This reaction not only represents the key point of entry of reduced nitrogen into the food chain but also embodies the formidable chemistry of breaking the N≡N triple bond under ambient conditions.

Four classes of nitrogenases have been identified to date.[1] The "classical" molybdenum (Mo) nitrogenase of *Azotobacter vinelandii* is composed of two component proteins, the iron (Fe) protein and the molybdenum−iron (MoFe) protein. The α_2-dimeric Fe protein is bridged by a single $[Fe_4S_4]$ cluster between the subunits and contains one ATP binding site per subunit, whereas the $\alpha_2\beta_2$-tetrameric MoFe protein contains two unique clusters per $\alpha\beta$-subunit pair: the P-cluster ($[Fe_8S_7]$), which is located at the α/β-subunit interface, and FeMoco ($[MoFe_7S_9X$-homocitrate$]$)[2] , which is situated within the α-subunit (*8, 9*). Substrate reduction of nitrogenase involves complex association and dissociation between the Fe protein and the MoFe protein, and the sequential, interprotein transfer of electrons from the $[Fe_4S_4]$ cluster of Fe protein to the P-cluster and, eventually, FeMoco of MoFe protein, where substrate is reduced (Figure 1).

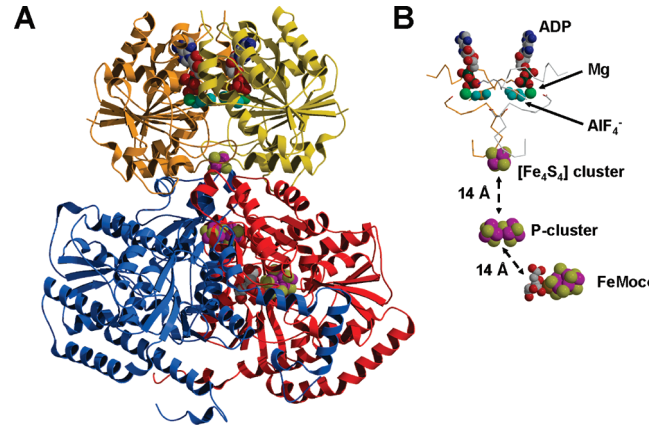

FIGURE 1: X-ray crystal structure of half of the ADP·AlF_4^- stabilized Fe protein−MoFe protein complex (A) and the relative positions of components in the complex that are involved in the electron flow (B) (*10*). The identical subunits of Fe protein are colored orange and yellow, and the α- and β-subunits of MoFe protein are colored red and blue, respectively.

There is great interest in decoding the assembly mechanism of MoFe protein and, particularly, its unique P-cluster and FeMoco, which are not only biologically important but also chemically unprecedented.[3] Following an introduction about the properties of *A. vinelandii* MoFe protein, this review will focus on recent advances in understanding the assembly of this MoFe protein, with an emphasis on studies that provide structural or spectroscopic insights into this process.

[†] This work was supported by NIH Grant GM-67626 (M.W.R.).

* To whom correspondence should be addressed. Y.H.: e-mail, yilinh@uci.edu; phone, (949) 824-4737; fax, (949) 824-8551. M.W.R.: e-mail, mribbe@uci.edu; phone, (949) 824-9509; fax, (949) 824-8551.

[1] Four classes of nitrogenases have been described. They are the molybdenum nitrogenase, the vanadium nitrogenase, the iron-only nitrogenase, and the nitrogenase from *Streptomyces thermoautotrophicus*. The major distinctive feature of the first three classes of nitrogenases, which are otherwise very similar, is the heterometal atom in the active site of the metal cluster (molybdenum, vanadium, and iron, respectively). The fourth nitrogenase is superoxide-dependent and apparently different from the other nitrogenase classes (*7*). Most of the current knowledge concerning the mechanism of nitrogenases is based on studies of the molybdenum nitrogenase; hence, this enzyme will be the focus of discussion in this article.

[2] The identity of X is unknown, but it is considered to be N, C, or O (*8*).

[3] Recently, significant progress has been made in the chemical synthesis of P-cluster topologs (*11−17*).

10.1021/bi7025003 CCC: $40.75
Published on Web 03/04/2008

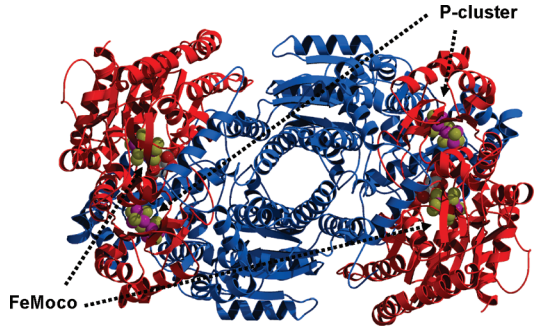

FIGURE 2: X-ray crystal structure of the $\alpha_2\beta_2$-tetrameric MoFe protein of *A. vinelandii* (*8, 9*). The α- and β-subunits of MoFe protein are colored red and blue, respectively. The positions of the P-cluster and FeMoco are indicated.

PROPERTIES OF MoFe PROTEIN

The MoFe protein of *A. vinelandii* is an $\alpha_2\beta_2$-tetramer of ~230 kDa, and its α-subunit (~55 kDa) and β-subunit (~59 kDa) are encoded by the *nifD* and *nifK* genes, respectively. The protein consists of a pair of αβ-dimers related by a molecular 2-fold rotation axis (Figure 2) (*8, 9*). Each of the homologous α- and β-subunits comprises three domains, designated αI, αII, and αIII and βI, βII, and βIII, respectively, all of which exhibit a parallel β-sheet/α-helical type of polypeptide fold. The P-cluster is located between domains αI and βI, whereas FeMoco occupies a cavity formed among domains αI−αIII.

P-Cluster. The P-cluster is found at the interface between the α- and β-subunit, 10 Å below the surface of the protein (*8, 9*). When MoFe protein is isolated in the presence of excess dithionite, its P-cluster exists in a diamagnetic state (designated P^N) (*18, 19*). All of the Fe atoms of the P^N state are believed to be ferrous. The P^N state of the P-cluster can be two-electron oxidized to the P^{2+} state (designated P^{OX}) with oxidants like indigo disulfonate (IDS) (*20*). This stable S = integer (3 or 4) state can be recognized by a $g = 11.8$ signal in the parallel mode EPR (*19, 21*). Both oxidation states of the P-cluster (Figure 3A,B) contain eight Fe and seven S atoms, which are covalently coordinated to the MoFe protein by six cysteinyl ligands, three from the α-subunit ($Cys^{\alpha62}$, $Cys^{\alpha88}$, and $Cys^{\alpha154}$) and three from the β-subunit ($Cys^{\beta70}$, $Cys^{\beta95}$, and $Cys^{\beta153}$). In both cases, $Cys^{\alpha62}$, $Cys^{\alpha154}$, $Cys^{\beta70}$, and $Cys^{\beta153}$ coordinate one Fe atom each, whereas $Cys^{\alpha88}$ and $Cys^{\beta95}$ coordinate two Fe atoms each (*9, 22, 23*). However, P^N and P^{OX} are structurally different in that one-half of the P-cluster in the P^{OX} state is present in a more open conformation. The interconversion between P^N and P^{OX} involves two Fe atoms of the P-cluster, and changes in the core structure of the cluster are accompanied by changes in the ligation between the cluster and the protein (*23*). Two additional protein ligands are present in the P^{OX} state; one is the Oγ atom of $Ser^{\beta188}$ that coordinates the same Fe atom as the cysteinyl group of $Cys^{\beta153}$, and the other is the $Cys^{\alpha88}$ that coordinates an Fe atom with a backbone amide nitrogen ligand in addition to providing a cysteinyl ligand to the same Fe atom (*23*).

FeMoco. FeMoco is located within the α-subunit of MoFe protein, 14 Å from the P-cluster. It can be studied when it is buried within the MoFe protein or extracted into *N*-methylformamide (NMF) (*2, 24, 25*). FeMoco can undergo reversible one-electron oxidation and reduction (*1*), and it is generally considered as the site of substrate reduction. The overall stoichiometry of FeMoco is 1Mo:7Fe:9S:1homocitrate, and it can be viewed as a $[Fe_4S_3]$ and a $[MoFe_3S_3]$ cluster bridged by three inorganic sulfide atoms (Figure 3C) (*8, 9, 25*). In addition, high-resolution (1.16 Å) X-ray structural analysis of *A. vinelandii* MoFe protein reveals the presence of a μ_6-interstitial light atom X in the center of FeMoco (*8*).[2] The identity of this atom has remained as one of the focal points of ongoing research (*26–30*) because of its promising relevance to substrate reduction (*5*). The core charge of FeMoco is proposed to be +1 or +3 in the resting state (*31, 32*), yet isolated FeMoco is known to be anionic (*25*). The overall negative charge of FeMoco is supplied by homocitrate, an organic terminal ligand of Mo, which is −4 if the OH group is deprotonated. FeMoco is ligated to the α-subunit of MoFe protein by just two ligands, $His^{\alpha442}$ at the Mo/homocitrate end and $Cys^{\alpha275}$ at the opposite end.

ASSEMBLY OF MoFe PROTEIN

Assembly of MoFe protein is arguably one of the most complex processes in the field of bioinorganic chemistry, requiring, at least, the participation of *nifS*, *nifU*, *nifB*, *nifE*, *nifN*, *nifV*, *nifQ*, *nifZ*, *nifH*, *nifD*, and *nifK* gene products (*33*). Multiple events occur during this process, including the biosynthesis of clusters, the incorporation of clusters into the polypeptide matrices, and the coordination of these events that eventually leads to the formation of a mature protein. Although previous genetically derived information contributed a great deal to the identification of factors involved in MoFe protein assembly, the exact function of these factors and the precise sequence of events have remained unclear until recently, when characterization of a number of assembly-related intermediates provided significant insight into this biosynthetic "black box". A refined mechanism of MoFe protein assembly can be proposed on the basis of these intermediates (Figure 4), which consists of (1) "*ex situ*" assembly of FeMoco on NifEN, (2) incorporation of FeMoco into MoFe protein, (3) "*in situ*" assembly of the P-cluster on MoFe protein, and (4) stepwise assembly of MoFe protein.

Ex Situ Assembly of FeMoco (Figure 4, 1). Biosynthesis of FeMoco occurs in a manner independent of the production of MoFe protein polypeptides (hence the term *ex situ*, which refers to the biosynthesis of FeMoco outside of the target MoFe protein) (*34*). Largely on the basis of genetic evidence, FeMoco biosynthesis is likely launched by NifUS (*nifU* and *nifS* gene products), which mobilizes Fe and S for the assembly of small Fe/S fragments (*35–39*). These small Fe/S fragments are subsequently transferred to NifB (*nifB* gene product) and further processed into a FeMoco "core" that potentially contains all necessary Fe and S for the generation of a mature cofactor (*33, 40*). The FeMoco core is then transferred to NifEN (*nifE* and *nifN* gene products) and undergoes additional rearrangement before its delivery to the MoFe protein (*33, 41, 42*). Thus, the flow of Fe and S through the biosynthetic pathway of FeMoco is likely as follows: NifUS → NifB → NifEN → MoFe protein (*nifD* and *nifK* gene products) (*33*). Other key players in FeMoco biosynthesis include NifV (*nifV* gene product), the homocitrate synthase that is in charge of supplying homocitrate for FeMoco biogenesis; NifQ (*nifQ* gene product), a protein factor that is potentially responsible for mobilizing Mo for FeMoco assembly; and Fe protein (*nifH* gene product), the

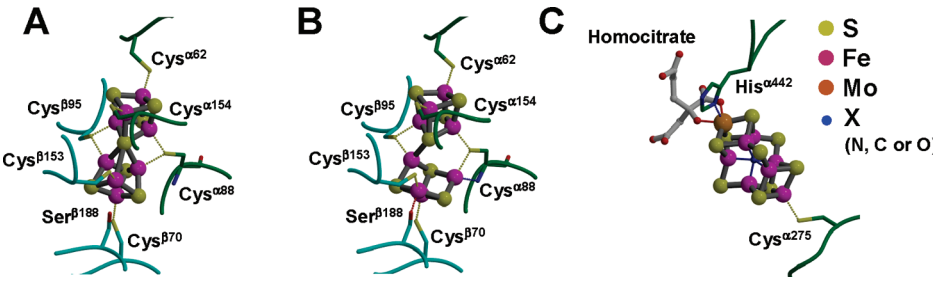

FIGURE 3: Structures of P^N (A) and P^{OX} (B) states of the P-cluster (*20, 21*) and FeMoco (C) (*8*).

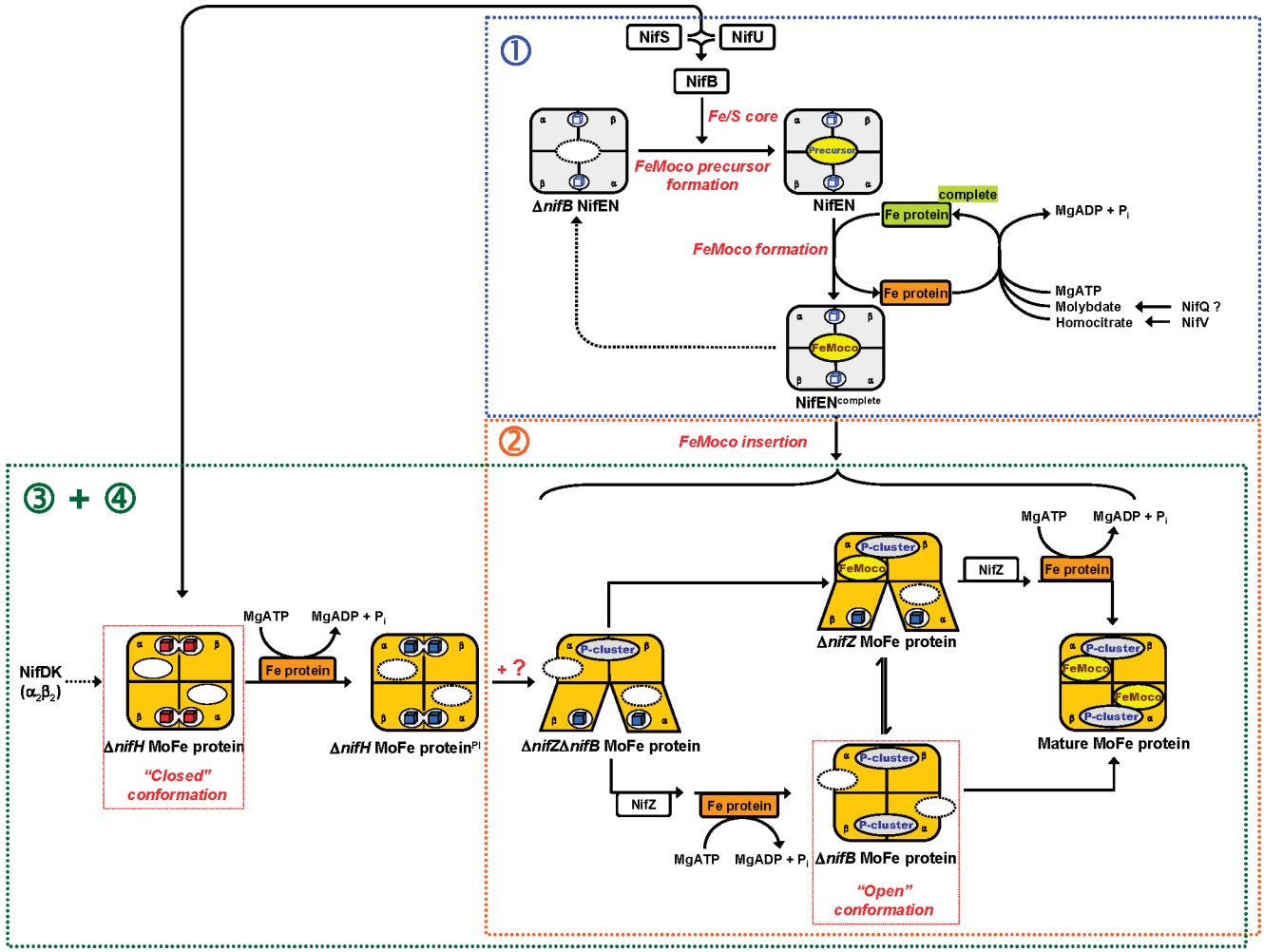

FIGURE 4: Refined model of the assembly of nitrogenase MoFe protein. (1) *Ex situ* assembly of FeMoco on NifEN, which involves a series of events leading to the conversion of the precursor (as in NifEN) to "FeMoco" (as in $NifEN^{complete}$) upon addition of Mo and homocitrate by Fe protein/MgATP (as in Fe $protein^{complete}$). (2) Insertion of FeMoco into MoFe protein, which involves the concomitant conversion of the FeMoco binding site to an accessible conformation upon formation of the P-cluster, the direct transfer of FeMoco from NifEN to MoFe protein by protein–protein interactions, and the insertion of FeMoco into its binding site through a positively charged funnel. (3) and (4) *In situ* assembly of the P-cluster on MoFe protein and concurrent stepwise assembly of MoFe protein, which involve the sequential conversion of paired $[Fe_4S_4]$-like clusters to $[Fe_8S_7]$ P-clusters, one at a time, and the concomitant assembly of MoFe protein upon P-cluster formation and FeMoco insertion, one $\alpha\beta$-subunit half prior to the other. Maturation of the P-cluster involves the processing of the $[Fe_4S_4]$-like clusters (as in Δ*nifH* MoFe protein) into a more reduced form (as in Δ*nifH* MoFe $protein^{PI}$) by Fe protein/MgATP before the formation of the first P-cluster (as in Δ*nifZ*Δ*nifB* MoFe protein) through coupling of $[Fe_4S_4]$-like clusters. The second pair of $[Fe_4S_4]$-like clusters is forced into an unfavorable conformation for coupling by the assembly of the first P-cluster and requires the sequential actions of NifZ and Fe protein/MgATP for maturation. At this point, depending on the availability of FeMoco and the rate at which FeMoco is inserted, the second P-cluster is formed either before (as in Δ*nifB* MoFe protein) or after (as in Δ*nifZ* MoFe protein) the insertion of FeMoco into the first $\alpha\beta$-subunit half.

catalytic electron donor to MoFe protein that is also implicated in FeMoco maturation (*33, 43, 44*).

The participation of NifU, NifS, and NifB in the early assembly steps of FeMoco was originally established by deletion analyses of the respective encoding genes for these proteins (*45*). Recently, it was reported that FeMoco could be synthesized *in vitro* in an assay containing purified NifB and NifEN (*46*) and that NifB might act as a SAM-dependent enzyme during the synthesis of FeMoco (*47*). Currently, no spectroscopic or structural evidence is available that is directly indicative of the nature of cluster species rendered by the biosynthetic events prior to the intervention of NifEN.

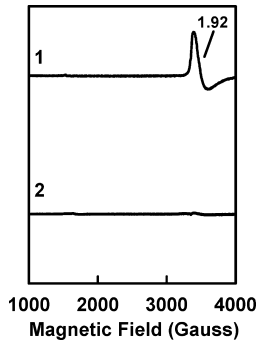

FIGURE 5: EPR spectra of (1) "unprocessed" NifEN (*48*) and (2) "processed" NifEN^{complete} (*34*) in the IDS-oxidized state.

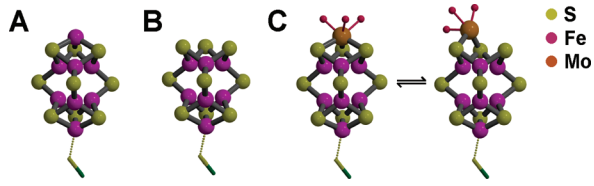

FIGURE 6: Fe_8 (A) and Fe_7 (B) model of the NifEN-bound FeMoco precursor (*50*) and model of NifEN-bound "FeMoco" (C). In all models, S is shown as the ligand to one of the terminal Fe atoms, as the Cys residue that ligates FeMoco in the MoFe protein is conserved in the NifE primary sequence. The disordered Mo environment in panel C is indicated by equilibrium between two plausible conformations of NifEN-bound FeMoco.

Nevertheless, NifB undoubtedly plays a considerable role in synthesizing a FeMoco core either prior to its transfer to NifEN or upon its interaction with NifEN, as NifEN isolated from *nifB*-deletion background is free of any biosynthetic intermediate of FeMoco, whereas NifEN isolated from *nifB*-intact background contains a FeMoco-like cluster (see below) (*48*). The eventual result of *nifB* deletion is the accumulation of a FeMoco-deficient form of MoFe protein (designated Δ*nifB* MoFe protein). Such a MoFe protein has an "open" FeMoco site that is readily accessible to FeMoco and, therefore, can be used to monitor the formation of FeMoco by *in vitro* FeMoco biosynthesis assays (see below).

The function of NifEN as a scaffold protein for further processing of the FeMoco core was initially proposed on the basis of a significant level of sequence identity between NifEN and MoFe protein, which has led to the hypothesis that NifEN contains cluster binding regions that are analogous to the P-cluster and FeMoco sites in the MoFe protein (*33, 41, 42, 49*). While the P-cluster analogue in NifEN was determined earlier to be a $[Fe_4S_4]$ type of cluster (*42*), the FeMoco counterpart in the protein has remained unidentified until the recent characterization of a NifEN complex isolated from *nifB*-intact yet *nifHDK*-deficient background. The absence of *nifDK*-encoded MoFe protein (the terminal acceptor of FeMoco) and *nifH*-encoded Fe protein (an essential factor for FeMoco maturation) allows the accumulation of a precursor form of FeMoco on NifEN. This NifEN-bound precursor contains no Mo and exhibits a unique $g = 1.92$ EPR signal in the IDS-oxidized state (Figure 5) (*48*). More excitingly, Fe K-edge XAS analysis reveals that the precursor is a Mo-free analogue of FeMoco and not one of the more commonly suggested cluster types based on the standard $[Fe_4S_4]$ architecture (*50*). Both the Fe_8 model (Figure 6A) and the Fe_7 model (Figure 6B) of the precursor resemble FeMoco with slightly elongated interatomic distances (*33*). This finding suggests that, instead of following the previously postulated mechanism that involves the coupling of $[Fe_4S_3]$ and $[MoFe_3S_3]$ subclusters, FeMoco is assembled by the formation of the Fe/S core prior to the insertion of the heterometal.

The precursor on NifEN undergoes further transformation upon incubation with Fe protein, MgATP, MoO_4^{2-}, and homocitrate (*34*). NifEN reisolated after such treatment (designated NifEN^{complete}) contains Mo, as opposed to the untreated NifEN (designated NifEN), and it no longer exhibits the IDS-oxidized, $g = 1.92$ feature (Figure 5) that is characteristic of the Mo-free precursor (*34*). Furthermore, NifEN^{complete} can serve as a FeMoco donor that directly activates the FeMoco-deficient Δ*nifB* MoFe protein, suggesting that (1) both Mo and homocitrate are inserted into the precursor while it is still bound to NifEN and (2) the resulting fully complemented cluster is transferred from NifEN to MoFe protein by direct protein–protein interactions (*34*). Fe and Mo K-edge XAS/EXAFS studies of the NifEN^{complete}-bound cluster show that the FeMoco on NifEN^{complete} (Figure 6C) closely resembles the FeMoco on MoFe protein (Figure 3C), except for a significant amount of disorder in the Mo environment that likely results from the asymmetric coordination of Mo in NifEN as compared to that in MoFe protein (*34*). This observation indicates a final "touch-up" of the FeMoco structure through ligand coordination at its target site in MoFe protein.[4]

The observation that cluster conversion is completed prior to its exit from NifEN not only allows an accurate assessment of the biosynthetic events hosted by NifEN but also suggests a significant role of Fe protein in this process. Fe protein reisolated after incubation with MgATP, MoO_4^{2-}, homocitrate, and NifEN (designated Fe protein^{complete}) is capable of activating the Δ*nifB* MoFe in combination with NifEN (*53*). This observation indicates that Fe protein^{complete} carries Mo and homocitrate, which can be inserted into the precursor on NifEN for the formation of a fully complemented cluster that subsequently activates the Δ*nifB* MoFe protein (*53*). The concomitant hydrolysis of MgATP is absolutely required for the "loading" of Mo and homocitrate onto the Fe protein, for substitutions of ATP with ADP or nonhydrolyzable ATP analogues, or wild-type Fe protein with variant Fe proteins defective in MgATP hydrolysis, result in the inability of Fe protein to deliver Mo and homocitrate to NifEN (*53*). Comparative Mo K-edge XAS analysis of Fe protein^{complete} and free molybdate shows an edge shift of ~2.3 eV, indicating that the Mo associated with the Fe protein^{complete} is modified from its supplied form (*53*). Furthermore, there is an additional ~0.5 eV edge shift if homocitrate is omitted during the preparation of Fe protein^{complete}, suggesting the presence of homocitrate and its impact on the Mo environment in Fe protein^{complete} (*53*).

Incorporation of FeMoco into MoFe Protein (Figure 4, 2). Upon completion of its assembly on NifEN, FeMoco is transferred to and inserted in MoFe protein through a complicated mechanism. It has been suggested previously that the delivery of FeMoco from NifEN to MoFe protein is mediated by a carrier protein, such as NifX (*nifX* gene product), NifY (*nifY* gene product), or NafY (*nafY* gene

[4] A Mo-containing cluster has been identified on NifEN, which may offer an alternative route of FeMoco assembly (*50, 51*).

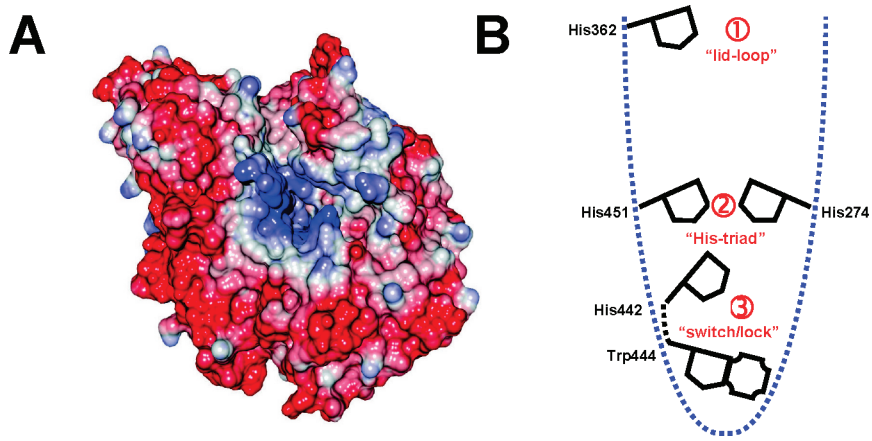

FIGURE 7: (A) Electrostatic surface potential representation of the Δ*nifB* MoFe protein (*60*). Negative, positive, and neutral potentials are colored red, blue, and gray, respectively. (B) Schematic representation of the positively charged funnel (blue dashed line) of the Δ*nifB* MoFe protein. Highlighted are key areas for FeMoco insertion: (1) lid loop, formed by residues α353−α364, among which His$^{\alpha 362}$ is the residue that is located at the tip of the loop; (2) His triad, formed by His$^{\alpha 274}$, His$^{\alpha 442}$, and His$^{\alpha 451}$; and (3) switch/lock, formed by His$^{\alpha 442}$ and Trp$^{\alpha 444}$ (*38*).

product), and that this carrier protein interacts with the MoFe protein ($\alpha_2\beta_2$) in a manner similar to that of the additional γ-subunit of the *Klebsiella pneumoniae* MoFe protein ($\alpha_2\beta_2\gamma_2$) during the transfer of FeMoco (*33, 54–56*).

However, the absolute requirement of such a FeMoco carrier was precluded by the previous observation of unaffected nitrogen fixing ability of the host upon deletions of carrier-encoding genes and the recent finding of direct FeMoco transfer between NifEN and MoFe protein upon protein–protein interactions (*34*). Sequence comparison between NifEN and MoFe protein reveals that certain residues that either provide a covalent ligand or tightly pack FeMoco within the polypeptide matrix of MoFe protein are not duplicated in the corresponding NifEN sequence. It is possible, therefore, that the respective cluster sites in NifEN and MoFe protein are brought into the proximity of each other, which allows the subsequent "diffusion" of FeMoco from its biosynthetic site in NifEN (low-affinity site) to its binding site in MoFe protein (high-affinity site). On the other hand, although the transfer of FeMoco can occur without a carrier protein, it may involve accessory factors that further improve the efficiency of this process. Thus, the factors previously hypothesized as FeMoco carriers may instead act as regulatory elements in FeMoco synthesis, post-translational modifiers that fine-tune the key residue(s) in the protein(s) for cluster formation, or chaperones that stabilize the protein complex and/or reposition the proteins in a favorable orientation for FeMoco transfer. Recently, one such factor, NifX, has been reported to participate in FeMoco assembly in a chaperone-like function (*57, 58*). In addition to the *nif*-specific accessory proteins, the well-established chaperone GroEL has also been shown to facilitate FeMoco insertion, although it is not clear if GroEL works alone or together with GroES in this process (*59*).

Upon its delivery to MoFe protein, FeMoco interacts with a number of MoFe protein residues en route to its target location within the protein. Identification of these residues was assisted by studies of Δ*nifB* MoFe protein, a P-cluster-intact yet FeMoco-deficient form of MoFe protein that can be readily reconstituted by isolated FeMoco (*60*). Comparison of the crystal structures of Δ*nifB* and wild-type MoFe proteins has led to the discovery of a positively charged "funnel" in the αIII domain of Δ*nifB* MoFe protein that is of sufficient size to accommodate the insertion of the negatively charged FeMoco (Figure 7A) (*60*). This observation, along with the fact that Δ*nifB* MoFe protein can be fully reconstituted by isolated FeMoco, strongly points to the physiological relevance of Δ*nifB* MoFe protein as a biosynthetic "snapshot" of MoFe protein immediately prior to FeMoco insertion. A closer inspection of the funnel reveals three distinct regions that are potentially important for FeMoco insertion. (1) The first is the "lid loop" (residues α353−α364), which potentially guides FeMoco to the insertion funnel. Among them, His$^{\alpha 362}$, which is located at the tip of the loop, could serve as a transient ligand for FeMoco at the entrance of the funnel (Figure 7B, 1). (2) The second is the "His triad" (His$^{\alpha 274}$, His$^{\alpha 442}$, and His$^{\alpha 451}$), which may provide a histidine-enriched, intermediary docking point for FeMoco during its journey through the funnel (Figure 7B, 2). (3) The third is the "switch/lock" (His$^{\alpha 442}$ and Trp$^{\alpha 444}$), which could secure FeMoco in its binding site by the bulky side chain of Trp$^{\alpha 444}$ following a swap in position between Trp$^{\alpha 444}$ and His$^{\alpha 442}$ at the bottom of the funnel (Figure 7B, 3) (*33, 60*). The participation of these residues in FeMoco insertion has been confirmed by mutational analyses that demonstrate a specific and substantial reduction in the level of FeMoco incorporation upon removal of the positive charge, ligand capacity, or steric effect at the respective positions (*61–63*). Furthermore, FeMoco insertion is accompanied by a considerable amount of structural rearrangement of MoFe protein. Consistent with the structurally confirmed "open" conformation of the αIII domain in Δ*nifB* MoFe protein (*60*), the SAXS-derived R_g value of the Δ*nifB* MoFe protein (42.4 Å) is slightly yet reproducibly larger than that of the wild-type MoFe protein (40.2 Å) (*64*), suggesting that Δ*nifB* MoFe protein has a more "relaxed" conformation than its wild-type counterpart. Considering that the Δ*nifB* MoFe protein is likely the biosynthetic intermediate right before the fully assembled MoFe protein, these observations indicate that MoFe protein undergoes a "compacting" conformational change upon FeMoco insertion.

In Situ Assembly of the P-Cluster (Figure 4, 3). On the basis of genetic evidence, biosynthesis of the P-cluster, like that of FeMoco, starts with the action of NifUS (*45*).

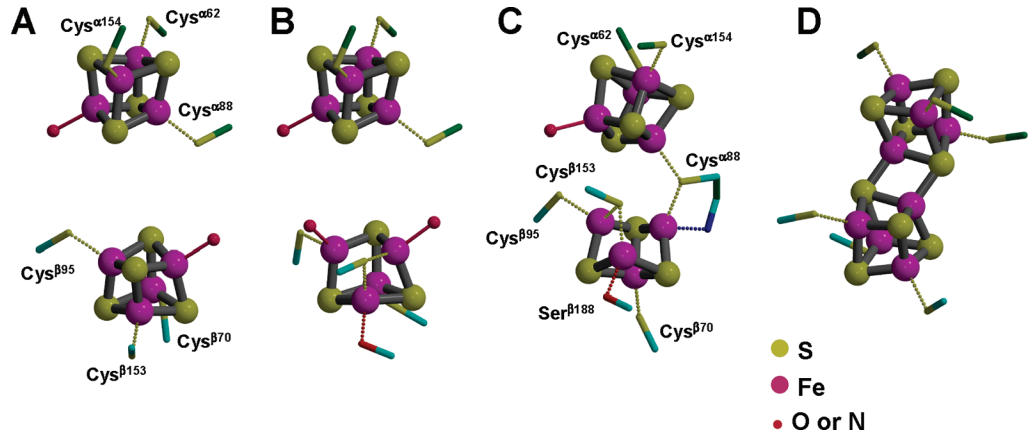

FIGURE 8: Structural models of the MoFe protein-bound P-cluster precursor (*67*). The cluster likely consists of two [Fe_4S_4] centers localized on the α- and *β*-subunit and exists either as two completely separate sites (A and B) or as two distinct Cys-ligated (C) or edge-bridged (D) fragments. Assignment of Cys ligands is based on comparison of the orientations of the precursor and P-cluster. Additionally, panel A, B, or C contains at least one O/N ligand (red).

However, further processing of small, NifUS-generated Fe/S fragments into a mature P-cluster takes place within the MoFe protein (hence the term *in situ*, which refers to the maturation of the P-cluster within the MoFe protein). There is evidence that Fe protein is involved in P-cluster formation; however, the exact function of Fe protein in the process, as well as the nature of the P-cluster biosynthetic intermediate, has remained largely unknown.

Earlier attempts at extracting P-clusters from MoFe protein have resulted in the recovery of [Fe_4S_4] clusters that might represent the breakdown products of the P-cluster. This observation pointed to the possibility of P-cluster formation by [Fe_4S_4] fragments, an approach that has been attempted by synthetic chemists to generate Fe/S clusters of high nuclearity (for a review, see ref *65*). Biological evidence in this regard was obtained recently from the characterization of a MoFe protein isolated from the *nifH*-deletion background (designated Δ*nifH* MoFe protein). Like Δ*nifB* MoFe protein, Δ*nifH* MoFe protein is FeMoco-deficient due to the absence of *nifH*-encoded Fe protein that is required for FeMoco maturation (see *Ex Situ* Assembly of FeMoco). However, in contrast to Δ*nifB* MoFe protein, Δ*nifH* MoFe protein contains an unusual "P-cluster", displaying, in the dithionite-reduced state, an $S = {}^1/_2$ EPR signal that is characteristic of [Fe_4S_4] clusters (*66*). Fe K-edge XAS/EXAFS analysis reveals that the P-cluster in Δ*nifH* MoFe protein is composed of paired [Fe_4S_4]-like clusters, either separated or bridged (Figure 8) (*67*). VTVH-MCD analysis provides further support for the model of separated [Fe_4S_4] centers, showing that each [Fe_4S_4] pair contains a [Fe_4S_4]$^+$ cluster and a diamagnetic [Fe_4S_4]-like cluster which, upon IDS oxidation, becomes paramagnetic (*68*).

The paired [Fe_4S_4] clusters in Δ*nifH* MoFe protein represent a physiologically relevant precursor to the P-cluster, as Δ*nifH* MoFe protein can be fully activated, in crude extract, upon incubation with Fe protein, MgATP, dithionite, and isolated FeMoco (*69*). Given that Δ*nifH* MoFe protein contains precursors in place of the fully assembled P-clusters, it could represent an intermediate that occurs earlier than Δ*nifB* MoFe protein along the biosynthetic pathway. Comparative SAXS analysis of Δ*nifH*, Δ*nifB*, and wild-type MoFe proteins shows that the Δ*nifH* MoFe protein exists in the most extended conformation (R_g = 45.7 Å), followed by the Δ*nifB* MoFe protein (R_g = 42.4 Å), and then the wild-type MoFe protein (R_g = 40.2 Å) (*64*). The increase in the size of Δ*nifH* MoFe protein is correlated to an increase in the solvent accessibility of the P-cluster precursor Fe atoms and can be best modeled by a 6 Å gap at the α/*β*-subunit interface (Figure 9C) that is absent from the structure of either Δ*nifB* (Figure 9B) or wild-type (Figure 9A) MoFe protein. These results suggest that the coupling of P-cluster subclusters is accompanied by a conformational change in the MoFe protein that brings the α- and *β*-subunits together. Furthermore, maturation of the P-cluster not only affects the α/*β*-subunit interface but also has an impact on the FeMoco binding site within the α-subunit of MoFe protein. Upon incubation with Fe protein, MgATP, and the reductant, not only is the P-cluster precursor in the Δ*nifH* MoFe further processed (*70*), the protein (designated Δ*nifH* MoFe^{PI}) can also be activated to ~10% of the maximal activity, suggesting that, concomitant with the formation of the P-cluster, the FeMoco site is partially "opened" up, possibly upon the Fe protein-induced conformational changes. Thus, the *in situ* assembly of the P-cluster within MoFe protein triggers multiple events that eventually lead to the formation of a mature MoFe protein.

Stepwise Assembly of MoFe Protein (Figure 4, 4). One important aspect of MoFe protein assembly is the coordination of multiple events that occur during the process, including the timing of cluster synthesis and insertion and the order of subunit folding and rearrangement. While there is strong evidence supporting the concept that P-cluster formation precedes FeMoco insertion (see *In Situ* Assembly of the P-Cluster), little is known about how assembly events of the two α*β*-subunit halves are aligned.

Recently, a "half-assembled" form of MoFe protein was isolated from the *nifZ*-deletion background (designated Δ*nifZ* MoFe protein), which contains a P-cluster and a FeMoco in one α*β*-subunit dimer and a P-cluster precursor and a vacant FeMoco site in the other (*71*). The P-cluster species in the "second" half comprises two [Fe_4S_4]-like clusters, as it exhibits the $S = {}^1/_2$ EPR signal that is very much similar to that displayed by the precursor in Δ*nifH* MoFe protein (*66, 71*). These observations suggest that (1) MoFe protein is assembled in a stepwise fashion, (2) completion of the "first" α*β*-half forces the "second" half into a conformation that

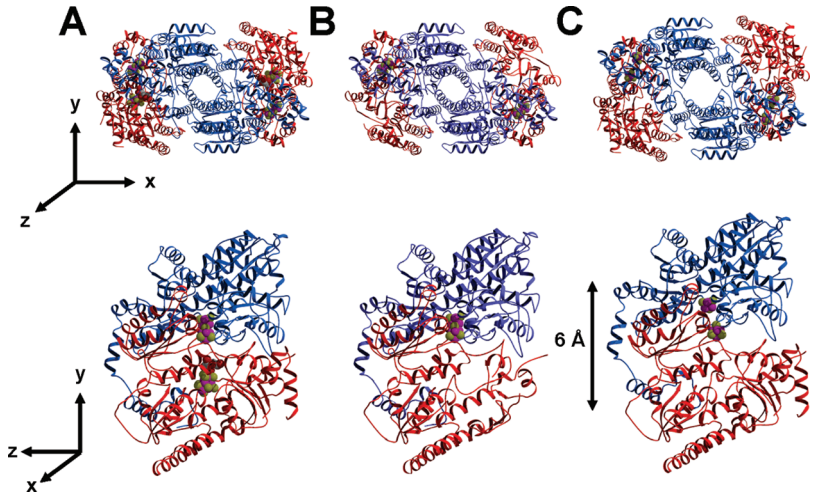

FIGURE 9: Ribbon diagrams of wild-type MoFe protein (A), Δ*nifB* MoFe protein (B), and the model that fits the SAXS data of the Δ*nifH* MoFe protein best (*64*) (C): (top) a complete $\alpha_2\beta_2$-heterotetramer and (bottom) a single $\alpha\beta$-heterodimer viewed end-on. The α- and β-subunits of MoFe protein are colored red and blue, respectively. The Δ*nifH* MoFe protein model was constructed from the wild-type MoFe protein structure by deletion of the FeMoco clusters, followed by a symmetric 6 Å translation of the α- and β-subunits about the *y*-axis.

does not allow proper coupling of the two [Fe_4S_4] fragments into a mature P-cluster, and (3) NifZ is specifically required for the formation of the second P-cluster, possibly through a chaperone-like function.

Subsequent studies of a MoFe protein isolated from the *nifZ*/*nifB*-double deletion background (designated Δ*nifZ*Δ*nifB* MoFe protein) allowed investigation of the maturation of the second P-cluster without the interference of FeMoco. Such a MoFe protein is FeMoco-deficient and contains one P-cluster in one $\alpha\beta$-half and one paired [Fe_4S_4]-like cluster in the other, as confirmed by EPR (*71*) and preliminary MCD studies (unpublished data). Consistent with the presence of a fully assembled P-cluster in the first half, Δ*nifZ*Δ*nifB* MoFe protein can be activated, without additional factors, to ~50% of the activity of the fully reconstituted Δ*nifB* MoFe protein (*71*). Upon incubation with NifZ and Fe protein/MgATP, Δ*nifZ*Δ*nifB* MoFe protein can be further activated to ~86% of the maximal activity. The additional ~36% increase in the level of activation suggests the conversion of a major portion of the precursor to the mature P-cluster in the second half of the protein, which is further backed up by EPR analysis that shows a decrease in the intensity of the precursor-associated $S = {}^1/_2$ signal and a concurrent increase in the magnitude of the P^{2+}-associated, $g = 11.8$ signal during this process (*72*). Furthermore, the action of NifZ is required prior to that of Fe protein/MgATP for the maturation of the second P-cluster, as Δ*nifZ*Δ*nifB* MoFe protein reisolated after incubation with NifZ alone can be activated by Fe protein/MgATP whereas Δ*nifZ*Δ*nifB* MoFe protein reisolated after incubation with Fe protein/MgATP cannot be activated by NifZ (*72*). The fact that Δ*nifZ*Δ*nifB* MoFe protein cannot be activated fully suggests that additional factors may be required along with NifZ for P-cluster formation. Such factors could be the products of *nifW* and *nifM* genes, both of which were juxtapositioned with the *nifZ* gene on the chromosome and implicated earlier in MoFe protein assembly.

In conclusion, there has been major progress in the elucidation of the biosynthetic mechanism of MoFe protein and its associated metal clusters in recent years. However, the job of piecing together this biological puzzle is far from finished. With regard to FeMoco assembly, the biosynthetic events that occur prior to NifEN and, in particular, those hosted by NifB remain largely unknown, whereas in the case of P-cluster assembly, the biogenic steps leading to the formation of the precursor, and its subsequent incorporation into the target site, are poorly understood. In addition, how key proteins interact with each other during cluster transfer, as well as what accessory factors are involved in every biosynthetic step, has not been well explored. A comprehensive understanding of this complex process relies on future biochemical, spectroscopic, and structural studies that unambiguously determine the mode of action of each biosynthetic component and the network of interactions among these components.

ACKNOWLEDGMENT

We acknowledge Dr. Benedikt Schmid (Friedrich-Alexander-University of Erlangen-Nürnberg, Nürnberg, Germany) for his help in generating Figures 1−3, 6, 8, and 9.

REFERENCES

1. Burgess, B. K., and Lowe, D. J. (1996) Mechanism of molybdenum nitrogenase. *Chem. Rev. 96*, 2983–3012.
2. Howard, J. B., and Rees, D. C. (1996) Structural basis of biological nitrogen fixation. *Chem. Rev. 96*, 2965–2982.
3. Smith, B. E. (1999) Structure, function, and biosynthesis of the metallosulfur clusters in nitrogenases. *Adv. Inorg. Chem. 47*, 159–218.
4. Rees, D. C., Tezcan, F. A., Haynes, C. A., Walton, M. Y., Andrade, S., Einsle, O., and Howard, J. B. (2005) Structural basis of biological nitrogen fixation. *Philos. Trans. R. Soc. London, Ser. A 363*, 971–984.
5. Howard, J. B., and Rees, D. C. (2006) How many metals does it take to fix N_2? A mechanistic overview of biological nitrogen fixation. *Proc. Natl. Acad. Sci U.S.A. 103*, 17088–17093.
6. Peters, J. W., and Szilagyi, R. K. (2006) Exploring new frontiers of nitrogenase structure and mechanism. *Curr. Opin. Chem. Biol. 10*, 101–108.
7. Ribbe, M., Gadkari, D., and Meyer, O. (1997) N_2-fixation by *Streptomyces thermoautotrophicus* involves a Mo-dinitrogenase and a Mn-superoxide oxidoreductase that couple N_2 reduction to the oxidation of superoxide produced from O_2 by a Mo-CO dehydrogenase. *J. Biol. Chem. 272*, 26627–26633.
8. Einsle, O., Tezcan, F. A., Andrade, S. L., Schmid, B., Yoshida, M., Howard, J. B., and Rees, D. C. (2002) Nitrogenase MoFe-

protein at 1.16 Å resolution: A central ligand in the FeMo-cofactor. *Science 297*, 1696–1700.
9. Kim, J., and Rees, D. C. (1992) Crystallographic structure and functional implications of the nitrogenase molybdenum iron protein from *Azotobacter vinelandii*. *Nature 360*, 553–560.
10. Schindelin, H., Kisker, C., Schlessman, J. L., Howard, J. B., and Rees, D. C. (1997) Structure of ADP·AlF_4^--stabilized nitrogenase complex and its implications for signal transduction. *Nature 387*, 370–376.
11. Hlavinka, M. L., Miyaji, T., Staples, R. J., and Holm, R. H. (2007) Hydroxide-promoted core conversions of molybdenum-iron-sulfur edge-bridged double cubanes: Oxygen-ligated topological P^N clusters. *Inorg. Chem. 46*, 9192–9200.
12. Berlinguette, C. P., Miyaji, T., Zhang, Y., and Holm, R. H. (2006) Precursors to clusters with the topology of the P^N cluster of nitrogenase: Edge-bridged double cubane clusters $[(Tp)_2Mo_2Fe_6S_8L_4]^z$: Synthesis, structures, and electron transfer series. *Inorg. Chem. 45*, 1997–2007.
13. Zhang, Y., and Holm, R. H. (2004) Structural conversions of molybdenum-iron-sulfur edge-bridged double cubanes and P^N-type clusters topologically related to the nitrogenase P-cluster. *Inorg. Chem. 43*, 674–682.
14. Zhang, Y., and Holm, R. H. (2003) Synthesis of a molecular $Mo_2Fe_6S_9$ cluster with the topology of the P^N cluster of nitrogenase by rearrangement of an edge-bridged $Mo_2Fe_6S_8$ double cubane. *J. Am. Chem. Soc. 125*, 3910–3920.
15. Zuo, J. L., Zhou, H. C., and Holm, R. H. (2003) Vanadium-iron-sulfur clusters containing the cubane-type $[VFe_3S_4]$ core unit: Synthesis of a cluster with the topology of the P^N cluster of nitrogenase. *Inorg. Chem. 42*, 4624–4631.
16. Ohki, Y., Ikagawa, Y., and Tatsumi, K. (2007) Synthesis of new [8Fe-7S] clusters: A topological link between the core structures of P-cluster, FeMo-co, and FeFe-co of nitrogenases. *J. Am. Chem. Soc. 129*, 10457–10465.
17. Ohki, Y., Sunada, Y., Honda, M., Katada, M., and Tatsumi, K. (2003) Synthesis of the P-cluster inorganic core of nitrogenases. *J. Am. Chem. Soc. 125*, 4052–4053.
18. Zimmermann, R., Orme-Johnson, W. H., Münck, E., Shah, V. K., Brill, W. I., Henzl, M. T., and Rawlings, J. (1978) Nitrogenase-X: Mössbauer and EPR studies on reversibly oxidized MoFe protein from *Azotobacter vinelandii* OP: Nature of iron centers. *Biochim. Biophys. Acta 537*, 185–207.
19. Surerus, K. K., Hendrich, M. P., Christie, P. D., Rottgardt, D., Orme-Johnson, W. H., and Münck, E. (1992) Mössbauer and integer-spin EPR of the oxidized P-clusters of nitrogenase: P^{ox} is a non-Kramers system with a nearly degenerate ground doublet. *J. Am. Chem. Soc. 114*, 8579–8590.
20. Watt, G. D., Burns, A., Lough, S., and Tennent, D. L. (1980) Redox and spectroscopic properties of oxidized MoFe protein from *Azotobacter vinelandii*. *Biochemistry 19*, 4926–4932.
21. Pierik, A. J., Wassink, H., Haaker, H., and Hagen, W. R. (1993) Redox properties and EPR spectroscopy of the P-clusters of *Azotobacter vinelandii* MoFe Protein. *Eur. J. Biochem. 212*, 51–61.
22. Chan, M. K., Kim, J., and Rees, D. C. (1993) The nitrogenase FeMo-cofactor and P-cluster pair: 2.2 Å resolution structures. *Science 260*, 792–794.
23. Peters, J. W., Stowell, M. H., Soltis, S. M., Finnegan, M. G., Johnson, M. K., and Rees, D. C. (1997) Redox-dependent structural changes in the nitrogenase P-cluster. *Biochemistry 36*, 1181–1187.
24. Shah, V. K., and Brill, W. J. (1977) Isolation of an iron-molybdenum cofactor from nitrogenase. *Proc. Natl. Acad. Sci. U.S.A. 74*, 3249–3253.
25. Burgess, B. K. (1990) The iron molybdenum cofactor of nitrogenase. *Chem. Rev. 90*, 1377–1406.
26. Hinnemann, B., and Norskov, J. K. (2003) Modeling a central ligand in the nitrogenase FeMo cofactor. *J. Am. Chem. Soc. 125*, 1466–1467.
27. Lovell, T., Liu, T. Q., Case, D. A., and Noodleman, L. (2003) Structural, spectroscopic, and redox consequences of central ligand in the FeMoco of nitrogenase: A density functional theoretical study. *J. Am. Chem. Soc. 125*, 8377–8383.
28. Dance, I. (2003) The consequences of an interstitial N atom in the FeMo cofactor of nitrogenase. *Chem. Commun. 3*, 324–325.
29. Vrajmasu, V., Münck, E., and Bominaar, E. L. (2003) Density functional study of the electric hyperfine interactions and the redox-structural correlations in the cofactor of nitrogenase. Analysis of general trends in Fe-57 isomer shifts. *Inorg. Chem. 42*, 5974–5988.
30. Yang, T. C., Maeser, N. K., Laryukhin, M., Lee, H. I., Dean, D. R., Seefeldt, L. C., and Hoffman, B. M. (2005) The interstitial atom of the nitrogenase FeMo-Cofactor: ENDOR and ESEEM evidence that it is not a nitrogen. *J. Am. Chem. Soc. 127*, 12804–12805.
31. Lee, H.-I., Hales, B. J., and Hoffman, B. M. (1997) Metal-ion valencies of the FeMo cofactor in CO-inhibited and resting state nitrogenase by Fe-57 Q-band ENDOR. *J. Am. Chem. Soc. 119*, 11395–11400.
32. Yoo, S. J., Angove, H. C., Papaefthymiou, V., Burgess, B. K., and Münck, E. (2000) Mössbauer study of the MoFe protein of nitrogenase from *Azotobacter vinelandii* using selective Fe^{57} enrichment of the M-centers. *J. Am. Chem. Soc. 122*, 4926–4936.
33. Dos Santos, P. C., Dean, D. R., Hu, Y. L., and Ribbe, M. W. (2004) Formation and insertion of the nitrogenase iron-molybdenum cofactor. *Chem. Rev. 104*, 1159–1173.
34. Hu, Y., Corbett, M. C., Fay, A. W., Webber, J. A., Hodgson, K. O., Hedman, B., and Ribbe, M. W. (2006) FeMo cofactor maturation on NifEN. *Proc. Natl. Acad. Sci. U.S.A. 103*, 17119–17124.
35. Frazzon, J., and Dean, D. R. (2002) Biosynthesis of the nitrogenase iron-molybdenum-cofactor from *Azotobacter vinelandii*. *Met. Ions Biol. Syst. 39*, 163–186.
36. Yuvaniyama, P., Agar, J. N., Cash, V. L., Johnson, M. K., and Dean, D. R. (2000) NifS-directed assembly of a transient [2Fe-2S] cluster within the NifU protein. *Proc. Natl. Acad. Sci. U.S.A. 97*, 599–604.
37. Agar, J. N., Yuvaniyama, P., Jack, R. F., Cash, V. L., Smith, A. D., Dean, D. R., and Johnson, M. K. (2000) Modular organization and identification of a mononuclear iron-binding site within the NifU protein. *J. Biol. Inorg. Chem. 5*, 167–177.
38. Dos Santos, P. C., Smith, A. D., Frazzon, J., Cash, V. L., Johnson, M. K., and Dean, D. R. (2004) Iron-sulfur cluster assembly: NifU-directed activation of the nitrogenase Fe protein. *J. Biol. Chem. 279*, 19705–19711.
39. Smith, A. D., Jameson, G. N. L., Dos Santos, P. C., Agar, J. N., Naik, S., Krebs, C., Frazzon, J., Dean, D. R., Huynh, B. H., and Johnson, M. K. (2005) NifS-mediated assembly of [4Fe-4S] clusters in the N- and C-terminal domains of the NifU scaffold protein. *Biochemistry 44*, 12955–12969.
40. Allen, R. M., Chatterjee, R., Ludden, P. W., and Shah, V. K. (1995) Incorporation of iron and sulfur from NifB cofactor into the iron-molybdenum cofactor of dinitrogenase. *J. Biol. Chem. 270*, 26890–26896.
41. Roll, J. T., Shah, V. K., Dean, D. R., and Roberts, G. P. (1995) Characteristics of NifNE *in Azotobacter vinelandii* strains: Implications for the synthesis of the iron-molybdenum cofactor of dinitrogenase. *J. Biol. Chem. 270*, 4432–4437.
42. Goodwin, P. J., Agar, J. N., Roll, J. T., Roberts, G. P., Johnson, M. K., and Dean, D. R. (1998) The *Azotobacter vinelandii* NifEN complex contains two identical [4Fe-4S] clusters. *Biochemistry 37*, 10420–10428.
43. Hoover, T. R., Robertson, A. D., Cerny, R. L., Hayes, R. N., Imperial, J., Shah, V. K., and Ludden, P. W. (1987) Identification of the V-factor needed for synthesis of the iron-molybdenum cofactor of nitrogenase as homocitrate. *Nature 329*, 855–857.
44. Zheng, L. M., White, R. H., and Dean, D. R. (1997) Purification of the *Azotobacter vinelandii* nifV-encoded homocitrate synthase. *J. Bacteriol. 179*, 5963–5966.
45. Dean, D. R., and Jacobson, M. R. (1992) Biochemical genetics of Nitrogenase, in *Biological Nitrogen Fixation* (Stacey, G., Burris, R. H., and Evans, H. J., Eds.) pp 763–834, Chapman & Hall, New York.
46. Curatti, L., Hernandez, J. A., Igarashi, R. Y., Soboh, B., Zhao, D., and Rubio, L. M. (2007) *In vitro* synthesis of the iron-molybdenum cofactor of nitrogenase from iron, sulfur, molybdenum, and homocitrate using purified proteins. *Proc. Natl. Acad. Sci. U.S.A. 104*, 17626–17631.
47. Curatti, L., Ludden, P. W., and Rubio, L. M. (2006) NifB-dependent *in vitro* synthesis of the iron-molybdenum cofactor of nitrogenase. *Proc. Natl. Acad. Sci. U.S.A. 103*, 5297–5301.
48. Hu, Y., Fay, A. W., and Ribbe, M. W. (2005) Identification of a nitrogenase iron-molybdenum cofactor precursor on NifEN complex. *Proc. Natl. Acad. Sci. U.S.A. 102*, 3236–3241.
49. Brigle, K. E., Weiss, M. C., Newton, W. E., and Dean, D. R. (1987) Products of the iron-molybdenum cofactor-specific biosynthetic genes, *nifE* and *nifN*, are structurally homologous to the products of the nitrogenase molybdenum-iron protein genes, *nifD* and *nifK*. *J. Bacteriol. 169*, 1547–1553.
50. Corbett, M. C., Hu, Y., Fay, A. W., Ribbe, M. W., Hedman, B., and Hodgson, K. O. (2006) Structural insights into a protein-bound

iron-molybdenum cofactor precursor. *Proc. Natl. Acad. Sci. U.S.A. 103*, 1238–1243.

51. George, S. J., Igarashi, R. Y., Piamonteze, C., Soboh, B., Cramer, S. P., and Rubio, L. M. (2007) Identification of a Mo-Fe-S cluster on NifEN by Mo K-edge extended X-ray absorption fine structure. *J. Am. Chem. Soc. 129*, 3060–3601.
52. Soboh, B., Igarashi, R. Y., Hernandez, J. A., and Rubio, L. M. (2006) Purification of a NifEN protein complex that contains bound molybdenum and a FeMo-Co precursor from an *Azotobacter vinelandii* Δ*nifHDK* strain. *J. Biol. Chem. 281*, 36701–36709.
53. Hu, Y., Corbett, M. C., Fay, A. W., Webber, J. A., Hodgson, K. O., Hedman, B., and Ribbe, M. W. (2006) Nitrogenase Fe protein: A moybdate/homocitrate insertase. *Proc. Natl. Acad. Sci. U.S.A. 103*, 17125–17130.
54. Homer, M. J., Paustian, T. D., Shah, V. K., and Roberts, G. P. (1993) The NifY product of *Klebsiella pneumoniae* is associated with apodinitrogenase and dissociates upon activation with the iron-molybdenum cofactor. *J. Bacteriol. 175*, 4907–4910.
55. White, T. C., Harris, G. S., and Orme-Johnson, W. (1992) Electrophoretic studies on the assembly of the nitrogenase molybdenum-iron protein from the *Klebsiella pneumoniae nifD* and *nifK* gene-products. *J. Biol. Chem. 267*, 24007–24016.
56. Homer, M. J., Dean, D. R., and Roberts, G. P. (1995) Characterization of the gamma-protein and its involvement in the metallocluster assembly and maturation of dinitrogenase from *Azotobacter vinelandii*. *J. Biol. Chem. 270*, 24745–24752.
57. Lukoyanov, D., Pelmenschikov, V., Maeser, N., Laryukhin, M., Yang, T. C., Noodleman, L., Dean, D. R., Case, D. A., Seefeldt, L. C., and Hoffman, B. M. (2007) Testing if the interstitial atom, X, of the nitrogenase molybdenum-iron cofactor is N or C: ENDOR, ESEEM, and DFT studies of the S = 3/2 resting state in multiple environments. *Inorg. Chem. 46*, 11437–11449.
58. Hernandez, J. A., Igarashi, R. Y., Soboh, B., Curatti, L., Dean, D. R., Ludden, P. W., and Rubio, L. M. (2007) NifX and NifEN exchange NifB cofactor and the VK-cluster, a newly isolated intermediate of the iron-molybdenum cofactor biosynthetic pathway. *Mol. Microbiol. 63*, 177–192.
59. Ribbe, M. W., and Burgess, B. K. (2001) The chaperone GroEL is required for the final assembly of the molybdenum-iron protein of nitrogenase. *Proc. Natl. Acad. Sci. U.S.A. 98*, 5521–5525.
60. Schmid, B., Ribbe, M. W., Einsle, O., Yoshida, M., Thomas, L. M., Dean, D. R., Rees, D. C., and Burgess, B. K. (2002) Structure of a cofactor-deficient nitrogenase MoFe protein. *Science 296*, 352–356.
61. Hu, Y., Fay, A. W., Schmid, B., Makar, B., and Ribbe, M. W. (2006) Molecular insights into nitrogenase FeMoco insertion: Trp 444 of MoFe protein α subunit locks FeMoco in its binding site. *J. Biol. Chem. 281*, 30534–30541.
62. Hu, Y., Fay, A. W., and Ribbe, M. W. (2007) Molecular insights into nitrogenase FeMoco insertion: The role of His362 of MoFe protein α subunit in FeMoco incorporation. *J. Biol. Inorg. Chem. 12*, 449–460.
63. Fay, A. W., Hu, Y., Schmid, B., and Ribbe, M. W. (2007) Molecular insights into nitrogenase FeMoco insertion: The role of His 274 and His 451 of MoFe protein α subunit. *J. Inorg. Biochem. 101*, 1630–1641.
64. Corbett, M. C., Hu, Y., Fay, A. W., Tsuruta, H., Ribbe, M. W., Hodgson, K. O., and Hedman, B. (2007) Conformational differences between *Azotobacter vinelandii* nitrogenase MoFe proteins as studied by small angle X-ray scattering. *Biochemistry 46*, 8066–8074.
65. Lee, S. C., and Holm, R. H. (2004) The clusters of nitrogenase: Synthetic methodology in the construction of weak-field clusters. *Chem. Rev. 104*, 1135–1158.
66. Ribbe, M. W., Hu, Y., Guo, M., Schmid, B., and Burgess, B. K. (2002) The FeMoco-deficient MoFe protein produced by a *nifH*-deletion strain of *Azotobacter vinelandii* shows unusual P-cluster features. *J. Biol. Chem. 277*, 23469–23476.
67. Corbett, M. C., Hu, Y., Naderi, F., Ribbe, M. W., Hedman, B., and Hodgson, K. O. (2004) Comparison of iron-molybdenum cofactor deficient nitrogenase MoFe proteins by X-ray absorption spectroscopy: Implications for P-cluster biosynthesis. *J. Biol. Chem. 279*, 28276–28282.
68. Broach, R. B., Rupnik, K., Hu, Y., Fay, A. W., Cotton, M., Ribbe, M. W., and Hales, B. J. (2006) VTVH-MCD spectroscopic study of the metal clusters in the Δ*nifB* and Δ*nifH* MoFe proteins of nitrogenase from *Azotobacter vinelandii*. *Biochemistry 45*, 15039–15048.
69. Tal, S., Chun, T. W., Gavini, N., and Burgess, B. K. (1991) The Δ*nifB* (or Δ*nifE*) FeMo cofactor-deficient MoFe protein is different from the Δ*nifH* protein. *J. Biol. Chem. 266*, 10654–10657.
70. Hu, Y., Corbett, M. C., Fay, A. W., Webber, J. A., Hedman, B., Hodgson, K. O., and Ribbe, M. W. (2005) Nitrogenase reactivity with P-cluster variants. *Proc. Natl. Acad. Sci. U.S.A. 102*, 13825–13830.
71. Hu, Y., Fay, A. W., Dos Santos, P. C., Naderi, F., and Ribbe, M. W. (2004) Characterization of *Azotobacter vinelandii nifZ*-deletion strains: Indication of stepwise MoFe protein assembly. *J. Biol. Chem. 279*, 54963–54971.
72. Hu, Y., Fay, A. W., Lee, C. C., and Ribbe, M. W. (2007) P-Cluster maturation on nitrogenase MoFe protein. *Proc. Natl. Acad. Sci. U.S.A. 104*, 10424–10429.

BI7025003